Acid and Alkaline Extracellular Proteases of *Yarrowia lipolytica*

David Ogrydziak

Abstract *XPR2* and *AXP1*, coding for alkaline (AEP) and acid (AXP) extracellular proteases, have been sequenced for several strains. For *XPR2*, the three sequenced strains are not closely related and produce significantly different levels of AEP, yet the coding sequences are identical, and there is only a single nucleotide difference in one promoter suggesting that host physiology, not promoter differences, determines AEP production. The possibility that pro-mAEP forms a dimer that can inhibit mature AEP (mAEP) proteolytic activity in *trans* is examined. AXP contains a predicted signal sequence and a 44 amino acid prepro-region. Activation involves pH-dependent autoprocessing that occurs extracellularly. *XPR2* UAS1 and UAS2 promoter elements have been identified and their roles in regulation explored. *Cis*-sequences and Rim pathway components involved in pH regulation of the proteases have been discovered and characterized. *YlOPT1* and *YLSSY5* are in a signaling pathway(s) regulating *AXP1* and *XPR2*, perhaps by sensing amino acids. Both pepsin-like (30 potentially secreted members) and subtilisin-like (16 potentially secreted members) gene families have undergone lineage-specific expansion compared to other yeast and filamentous fungi. To determine if expression of secretory pathway components is regulated in response to secretory demand, rapid AEP induction conditions and *XPR2* multicopy strains were developed. Changes in genomic transcription were measured when growth started to slow after AEP induction. For secretory pathway components, mostly repression was found. Possibly, their induction had occurred by the control time point, and the turning off of this short-term response at later time points appeared as repression.

D. Ogrydziak (✉)
Department of Food Science and Technology, University of California, One Shields Avenue, Davis, CA 95616, USA

Institute of Marine Resources, University of California, Davis, CA, USA
e-mail: dmogrydziak@ucdavis.edu

G. Barth (ed.), *Yarrowia lipolytica*, Microbiology Monographs 25,
DOI 10.1007/978-3-642-38583-4_2,

Contents

1 Introduction

Y. lipolytica alkaline and acid extracellular proteases were last extensively reviewed in an overall review of yeast extracellular proteases (Ogrydziak 1993).

Studies on the *Y. lipolytica* alkaline protease grew out of a project in which a yeast producing an extracellular protease(s) would solubilize fish proteins in a non-sterile process at acidic pH. *Y. lipolytica* was chosen because of its high extracellular proteolytic activity (Ahearn et al. 1968). When it became clear that the major protease secreted was an alkaline protease, the project changed to regulation and characterization of this protease.

Most likely all *Y. lipolytica* strains can produce an alkaline extracellular protease (AEP) . Various screens revealed substantial variation in AEP production between strains. Extensive inbreeding of *Y. lipolytica* strains has been done to improve their genetic manipulability. Strain CX161-1B, developed in Mortimer's laboratory, produced more AEP than strains developed in Heslot's laboratory, and wild strain W29 produced even more (see below).

XPR2 (coding for AEP) has been cloned and sequenced from three *Y. lipolytica* strains—NRRL Y-1094 (Davidow et al. 1987), CX161-1B (Matoba et al. 1988), and W29 (Nicaud et al. 1989). These strains are not closely related, but the coding sequences are identical. The promoter sequences of NRRL Y-1094 and W29 are identical and CX161-1B has one difference at position -404. Therefore, differences in AEP production probably reflect differences in host cell physiology, not promoter differences.

Surprisingly, *XPR2* from CLIB122, whose genome has been sequenced, has not been sequenced. CLIB122 contains *xpr2-322*, an *Apa*I deletion that removes amino acids 1–34 from the N-terminus of AEP (Barth and Gaillardin 1996). It was constructed with W29 *XPR2* DNA and integrated at the *Mlu*I site located over 900 bp upstream of the *Apa*I site. Therefore, most of the CLIB122 *XPR2* promoter

sequence and an unknown amount of the coding sequence, depending on where the crossover occurred for the "pop out," are derived from W29.

2 AEP Processing

AEP is co-translationally translocated into the endoplasmic reticulum (ER), the signal peptide cleaved, and the pro-region N-linked glycosylated to produce a 55-kDa polypeptide, the first precursor detected intracellularly in pulse-chase immunoprecipitation experiments (Ogrydziak 1993). This precursor is transported to the Golgi where nine N-terminal X-Ala, X-Pro dipeptides are removed by dipeptidyl aminopeptidase (DPAPase) to produce the 52 kDa precursor. Xpr6p cleavage after Lys.Arg at the end of the propeptide produces a 20 kDa propeptide and 32 kDa mature AEP (mAEP). S397A, an active site serine mutation that eliminates proteolytic activity, produces mAEP indicating that AEP proteolytic activity is not required for AEP processing (Matoba et al. 1997).

2.1 Signal Peptide Cleavage/Dipeptidyl Aminopeptidase Processing

Radiosequencing of the 55 kDa AEP precursor labeled with 3H-Leu and 35S-Met confirmed cleavage between Ala15 and Ala16 (Matoba et al. 1997). If signal peptide cleavage was after Ala15, Leu should be found at position 3 and there should be no Met signal. This is what was found. A 15 amino acid signal peptide was also found for the P17M AEP 55 kDa precursor (Yaver et al. 1992).

A recent review states that the AEP signal peptide is 13 amino acids long (Thevenieau et al. 2009). If signal peptide cleavage was after position 13, Leu should have been found at positions 1 and 5, and it was not. The possibility of an additional cleavage site(s) after Leu18 cannot be eliminated, as there is no Leu or Met for the next 26 amino acids in the pro-region. No 52 kDa AEP precursor was detected for A19V AEP (removal of only one dipeptide should occur), suggesting there is no downstream signal peptide cleavage site in-frame for DPAPase processing.

Analysis by SignalP 3.0 (Bendtsen et al. 2004) yields a prediction of maximum likelihood for the signal peptide cleavage site at Ala15-Ala16 using Neural Networks (NN) with Ala19-Ala20 as second most likely. Using Hidden Markov Models (HMM), maximum cleavage site probabilities were 0.605 between Pro21 and Ala22, 0.15 between Ala15 and Ala16, and 0.10 between Ala19 and Ala20. These predicted cleavage sites are all in the correct frame to allow removal of the downstream dipeptides by DPAPase.

The original review included evidence that DPAPase processing occurred in vivo (Ogrydziak 1993). N-terminal sequencing revealed that the 52 kDa precursor secreted by an *xpr6* mutant contained one species starting at the end of the dipeptide stretch and species starting one or two dipeptides upstream (Matoba and Ogrydziak 1989). Modifications of AEP (A19V and P17M), use of a DPAPase inhibitor proBoro, and expression of *XPR2* in *Saccharomyces cerevisiae* strains lacking both the Golgi and vacuolar DPAPases all demonstrated that mature AEP was still secreted when DPAPase processing was eliminated (Matoba et al. 1997). Therefore, Xpr6p processing was not dependent on DPAPase processing.

Deleting the *Y. lipolytica* Golgi DPAPase (YALI0B2838g) to determine effects on AEP processing is now possible. Unexpectedly, there does not appear to be a vacuolar DPAPase in CLIB 122.

2.2 Is Pro-mAEP a Dimer?

Wild-type strains secrete mAEP and propeptide but no AEP precursors (Matoba et al. 1988). The propeptide helps with the folding of AEP and inhibits its proteolytic activity; it was able in *trans* to enhance folding of a premature AEP construct lacking the pro-region (Fabre et al. 1992). If propeptide assistance in mAEP folding is intramolecular, this result suggests that the interaction occurs in the ER with unfolded or partially folded polypeptides. Inhibition of AEP activity by propeptide was demonstrated by the lack of proteolytic activity of the 52 kDa AEP precursor secreted by *xpr6* mutants (Enderlin and Ogrydziak 1994).

Secreted mAEP levels are significantly higher than for propeptide, suggesting propeptide is less stable. Propeptide degradation might start in the secretory pathway after Xpr6p cleavage. Or propeptide and mAEP might be secreted in equimolar amounts, perhaps as a non-covalently bound complex. Propeptide degradation would then begin when the complex dissociates.

Modification of this AEP processing model is proposed based on observations made decades ago. On skim milk (SKM) plates, segregants of crosses between wild-type and *xpr6* strains produced noncircular zones of clearing. If *xpr6* and wild-type segregants were adjacent, the edge of the zone of clearing between them was fairly straight. If the wild-type segregant was surrounded on four sides by *xpr6* segregants, it appears to form a square zone of clearing (Fig. 1).

Square zones strongly suggest that *xpr6* segregants are secreting something that interferes with clearing of SKM plates by mAEP. *xpr6-13* predominately secretes the 52 kDa pro-mAEP, lesser amounts of mAEP, and even less propeptide (Enderlin and Ogrydziak 1994). If only propeptide could inhibit mAEP activity, then any propeptide that diffused into the area normally cleared on SKM plates by an adjacent wild-type strain should be rapidly degraded, and no inhibition of clearing would be expected.

Square zones could be explained if pro-mAEP is more stable than propeptide to AEP degradation and if pro-mAEP can inhibit fully folded mAEP activity.

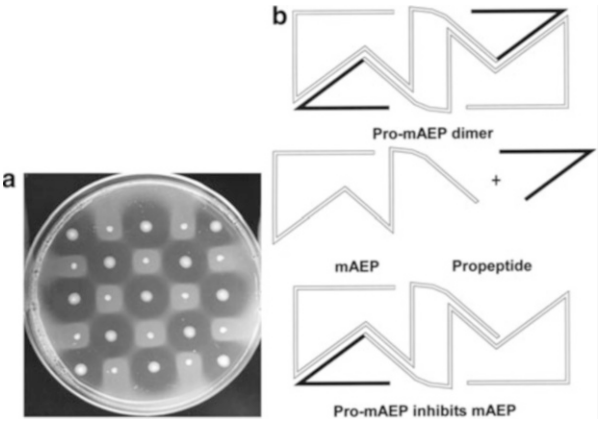

Fig. 1 (**a**) Wild-type and *xpr6-13* strains were toothpicked in an alternating pattern on SKM plates. Cleared zones appear *darker* because of the black background. (**b**) Schematic drawings representing the pro-mAEP dimer, mAEP and propeptide, and the pro-mAEP and mAEP complex. The pro-region is *black* and mature AEP *gray*. Adapted from Hu et al. (1996)

The front of mAEP diffusing from the wild type would meet the front of pro-mAEP diffusing from *xpr6*, and clearing on SKM plates would be inhibited in regions where the ratio of pro-mAEP to mAEP was sufficiently high, transforming the curved front of clearing into a relatively straight line.

For years, pro-mAEP inhibition of fully folded mAEP was not considered because it was assumed that the pro-region would already be involved in inhibiting the covalently attached mAEP region. AEP is a subtilisin-like protease, and Hu et al. (1996) showed that pro-subtilisin forms a dimer and that its assistance in folding and inhibition of the mature region could be intermolecular. This provided a model for how pro-mAEP could inhibit mAEP (Fig. 1). If pro-mAEP forms dimers and enhancement of folding and inhibition of protease activity by the pro-region can occur intermolecularly, then square zones can be explained.

Supernatant mixing experiments showed that pro-mAEP could inhibit mAEP. A 3:1 mixture of *xpr6-13* and wild-type supernatants yielded a 46 % decrease in AEP activity compared to fourfold dilution of the wild-type supernatant (unpublished results). If pro-mAEP was rapidly degraded by mAEP, such a significant inhibition of AEP activity might not be expected.

The *xpr6* mutants are slightly leaky. AEP activity measured by a casein hydrolysis assay was 0.1 % and 0.4 % of wild type for *xpr6-13* and *xpr6-25*, respectively (Ogrydziak and Mortimer 1977). Western blots of extracellular samples revealed no mAEP for a *Δxpr6* strain but what appears to be much greater than 0.1 % of wild-type levels of mAEP from *xpr6-13* (Enderlin and Ogrydziak 1994). Both *xpr6-13* and *xpr6-25* grow much faster on SKM plates than *Δxpr6*, consistent with some mAEP being produced and some proteolysis occurring. Inhibition of mAEP by pro-mAEP might explain why no zones of clearing are detected. There would be far more pro-mAEP than mAEP molecules, and if pro-mAEP were relatively stable, insufficient casein hydrolysis would occur to produce a zone of clearing.

Proving existence of the pro-mAEP dimer by examining samples from a *Δxpr6* strain under nondenaturing conditions would provide support for this new model. All previous samples were examined by SDS-PAGE, and a pro-mAEP dimer and

pro-mAEP/mAEP interactions would not have been detected. Reagents needed for more detailed studies of AEP inhibition by pro-mAEP and propeptide could be readily obtained—pro-mAEP from *Δxpr6* and propeptide from S397A.

3 AXP Processing

Since the original review, the N-terminal amino acid sequence of the extracellular acid protease from *Y. lipolytica* 148 was determined and *AXP1* cloned (Young et al. 1996). AXP is a 397 amino acid pepsin-like protein that includes a 44 amino acid prepro-region. The predicted amino acid sequence is identical to that of AXP from CLIB122. There is one silent nucleotide difference in the coding region, six nucleotide differences and a GTA insertion in the 5′ upstream region, and one nucleotide difference in the 3′ downstream region.

Predicted signal peptide cleavage occurs between Ala17 and Ala18. Unlike *XPR2*, the pro-region does not end in Lys.Arg; cleavage occurs between Phe44 and Ala45. This cleavage is due to pH-dependent autoprocessing (McEwen and Young 1998). In pulse-chase immunoprecipitation studies using an AXP-specific antibody, only a 42 kDa precursor but no mature AXP (39 kDa) was detected intracellularly. The 42 kDa precursor was secreted and at lower pHs (4.0 and 4.6) converted to mature AXP. This conversion happened extremely slowly, if at all, at pH 5.6 and 6.0. The 42 kDa precursor maturation was only slightly affected by the inhibitor pepstatin suggesting that autocatalytic activation was primarily intramolecular.

The mature region contains three potential N-linked glycosylation sites and the pro-region none. Mobility of the 42 kDa precursor on SDS-PAGE was unchanged for cells treated with tunicamycin indicating that no sites are used.

4 AEP Mode of Translocation

Yaver et al. (1992) found SRP-dependent co-translational translocation for wild-type AEP and SRP-independent posttranslational translocation for P17M—Pro to Met two amino acids after the signal peptide cleavage site.

For *S. cerevisiae*, proteins using the SRP-dependent pathway tend to have more hydrophobic signal peptides—HB12 (average hydrophobicity for 12 residues after the last positively charged residue of the n-region) values around 3.0 or more (Ng et al. 1996). Values around 2.0 or less were characteristic of proteins not using the SRP-targeting pathway. SRP-independent translocation of AEP would be predicted based on its HB 12 of 2.15. The P17M mutation, not in the signal peptide, did not change the signal peptide cleavage site and actually increased HB 16 slightly. Therefore, P17M translocation becoming SRP-independent posttranslational was unexpected.

SRP-dependent co-translational translocation could be restored by increasing hydrophobicity of the signal peptide (Matoba and Ogrydziak 1998). However, combining the A12P and P17M mutations had the same effect and did not increase hydrophobicity. Kinkiness was proposed as another factor(s) that may be important in translocation pathway choice. Structural models of the extended form of the wild-type N-terminus have a kink; P17M removes the kink caused by Pro17 resulting in a relatively straight structure. Addition of the A12P mutation restores the kink. Possibly the conformation of the signal peptide at the ribosome surface may affect the interaction with SRP. Less hydrophobic signal peptides might depend on the kink to approach SRP more closely more often to enhance interactions. These effects might only have been seen because of AEP signal peptide's short length and low average hydrophobicity. Not all the mutants fit this model; factors besides hydrophobicity and kinkiness can be important.

5 *XPR2* Regulation

Since the 1993 review, progress in understanding *XPR2* regulation has been substantial. The model was that partial derepression of AEP occurred when *Y. lipolytica* did not have access to preferred C-, N-, and S-sources. Protein in the medium had an inductive effect (Ogrydziak et al. 1977).

Deletion analysis of the *XPR2* promoter (p*XPR2*) identified *cis*-acting elements conferring high expression (Blanchin-Roland et al. 1994). A p*XPR2-lacZ* fusion integrated into the genome was used as a reporter for *XPR2* expression. Effects of deletions were measured in three media buffered with phosphate buffer (pH 6.8)—repressing (MMAm) containing glycerol (10 g/L), a good carbon source for *Y. lipolytica*, and ammonium sulfate (2 g/L); noninducing (YEg) with 1 % yeast extract and 0.1 % glucose; and inducing (YPDm) with 0.2 % yeast extract, 0.1 % glucose, and 5 % proteose peptone (PP). Two major UASs were identified—UAS1 between −822 and −769 and UAS2 between −208 and −140. Somewhat surprisingly, given the evolutionary distances, regulatory sequences similar to binding sites for *S. cerevisiae* transcription factors such as *GCN4* and *TUF/RAP1* were found in both UASs. In vivo footprinting revealed that proteins bound the UASs constitutively. The authors suggest that other regulatory proteins may modulate the activity of these bound proteins. Finally, *XPR2* expression was greatly reduced by deletion of both UASs, but regulation was retained.

The function of each UAS was defined more precisely using hybrid promoters consisting of p*XPR2* functional elements upstream of a minimal *LEU2* promoter (p*LEU2*) driving expression of the *lacZ* gene integrated into the genome (Madzak et al. 1999). UAS1A, corresponding to position -805 to -776 of p*XPR2*, carries *GCN4*-like and *TUF/RAP1*-like sites. UAS1B, corresponding to position -805 to -701, contains UAS1 and an adjacent region containing two imperfect repeats. UAS1B, and especially two copies of UAS1B (UAS1B2), enhanced β-galactosidase production more than UAS1A and UAS1A repeats on inducing

medium. UAS1B and UAS1B2 also increased activity on noninducing and repressing media indicating that the UAS1B hybrid promoters were less affected by environmental conditions. Levels were similar in YPDm and YEg suggesting absence of a peptone sensing element.

Three DNA fragments from UAS2 were tested. UAS2A (position -149 to -124) carries a decameric repeat that overlaps two sites identical to *Aspergillus nidulans* PacC site. UAS2C (position -126 to -106) partially overlaps a *GCN4*-like site and contains a site matching the *S. cerevisiae ABF1*-site consensus sequence. UAS2B (position -150 to -106) includes both UAS2A and UAS2C. UAS2A did not activate expression on YPDm, but in one orientation UAS2B caused a fivefold increase. Two copies of UAS2B caused more than an additive increase. UAS2C alone did not activate expression. Mutations in the *GCN4*-like or *ABF1*-like sites of UAS2B revealed that only the *ABF1*-like site is necessary for UAS activity.

Comparison of activity on YPDm at pH 6.8 and 4.0 revealed an effect for UAS2A and UAS2B but not UAS2C, suggesting that the decameric repeat containing the putative binding site for Rim101p/PacC regulator was important for pH control. *YlRIM101* context did not affect UAS1-driven expression but has major effects on UAS2-driven expression.

Madzak et al. (1999) concluded that UAS1 can increase activity in all media, especially as number of copies increase and that UAS1 is "poorly sensitive to repressing conditions." UAS2 seems to be involved in regulation by C- and N-sources and pH regulation. They proposed that at neutral or alkaline pH, YlRim101p is activated by a C-terminal truncation. This form can bind to PacC-like sites and activate p*XPR2* expression through UAS2. However, preferred C- and N-sources prevent this UAS2-driven expression suggesting that binding of another regulatory protein impairs YlRim101p activation.

Deletion of the UASs maintained regulation but at a much lower level, suggesting that they were not involved in regulation. But the hybrid promoters unexpectedly showed regulation similar to that of intact p*XPR2*. The authors attribute this to "compensation effects from other sequences still present in the deleted promoter" (Madzak et al. 1999).

The first search for *trans*-acting factors affecting AEP production concerned pH regulation (Otero and Gaillardin 1996). Strains with p*XPR2:lacZ* and p*XPR2:hph* fusions are white on YPD-X-Gal and hygromycin sensitive at pH 4.0. Nine stable mutants (PH1-9) that were blue and hygromycin resistant at pH 4.0 defined two RPH loci. The PH mutations seemed to affect only pH and not metabolic regulation of *XPR2*.

trans-acting regulatory mutations that prevent either p*XPR2*-driven expression under conditions of C- and N-limitation at pH 6.8, i.e., derepressing medium Y (1 % yeast extract), or force expression under repressing conditions were isolated (Lambert et al. 1997). To avoid *cis*-acting mutations, two reporters were used, production of AEP by *XPR2* and a p*XPR2-lacZ* fusion. Mutants that were Lac- and Xpr- on Y6.8 medium were considered nonderepressible. Seven recessive monogenic mutations defined four complementation groups—*PAL1–PAL4*. The *pal1*, *2*, and *3* mutants were transformed with a replicating vector library to find

genes that restore the Lac+ phenotype on Y-X-Gal 6.8. Plasmid pINA935 complemented only *pal2* mutations. pINA937 suppressed all four *pal* mutations and contained a truncated version of a gene designated *YlRIM101* based on homology to *S. cerevisiae* Rim101p and *A. nidulans* PacC.

YlRIM101p was shown to be absolutely required for transcriptional activation of *XPR2* at pH 6.8. *XPR2* expression at pH 4.0 was undetectable in the *YlRIM101* disruptant indicating that YLRim101p was not required for shutdown of expression in these conditions. C-terminal truncations of *YLRIM101* activated *XPR2* transcription.

A search was done for mutants (made using an mTnYl1-transposase library) that affected *AXP1* and/or *XPR2* expression to identify additional components of the pH signaling pathway and pH-independent regulators (Gonzalez-Lopez et al. 2002). To avoid *cis*-acting mutations, AEP and LacZ were assayed under p*XPR2* control and AXP and GusC under p*AXP1* control. In derepressing medium (Y) at pH 7.0, the parental strain made clear zones on SKM plates (Aep+) and turned blue on Y-X-Gal7 medium (Lac+). At pH 4.0, it cleared zones on BSA plates (Axp+) and turned blue on Y-Gluc4 medium (Gus+).

Around 190,000 transformants were screened. The four affecting only *XPR2* expression were *ScSIN3* homologs. Thirty mutations affecting only *AXP1* activity were not extensively characterized. The 89 mutations that affected expression of both proteases lead to identification of ten genes. Five were homologs of genes in the Rim pH signaling pathway. Five other genes were not involved in pH signaling—*OPT1*, *SSY5*, *VPS28*, *NUP85*, and *MED4*.

Possible roles of YlSin3p (component of a histone deacetylase), YlNup85p (nuclear pore protein), and YlMed4p (subunit of RNA polymerase II mediator complex) in extracellular protease regulation are presently unclear. YlVps28p is a component of the ESCRT-I complex, and there is now evidence suggesting that Rim and VPS pathways cooperate in ambient pH signaling possibly explaining its role in extracellular protease regulation (Blanchin-Roland et al. 2005).

Mutations affecting *YlOPT1* and *YLSSY5* nearly abolished *XPR2* and *AXP1* transcription but did not affect transcription of another pH-dependent gene. Gonzalez-Lopez et al. (2002) suggested that these genes may affect amino acid sensing. *OPT1* codes for a proton-coupled oligopeptide transporter in *S. cerevisiae*. Interestingly, the *OPT1*-related family of proteins is highly represented in *Y. lipolytica* (17 genes); the seven other yeast in Genolevures have only two to six genes (Sherman et al. 2009).

Possibly, the large number of potential oligopeptide transporters reflects *Y. lipolytica's* nutritional dependence on products of protein degradation by extracellular proteases. If several of these potential oligopeptide transporters are expressed, finding only *OPT1* mutations suggests that its primary role in protease regulation may not be oligopeptide transport. In *S. cerevisiae*, some of the numerous potential glucose transporters turn out to be glucose sensors (Ozcan et al. 1996). By analogy, perhaps YlOpt1p is an oligopeptide sensor, part of a signaling pathway that senses N-availability and/or indirectly inductive proteins/peptides in the medium.

In *S. cerevisiae*, Ssy5p is associated with Ptr3p and the permease-like Ssy1p in the plasma membrane. This complex detects the presence of extracellular amino acids and activates, by endoproteolytic processing, the membrane-bound transcription factor Stp1 to activate a signaling pathway leading to transcriptional induction of genes like AGP1—an amino acid permease (Abdel-Sater et al. 2004). Ssy5p has been shown to be the endoprotease responsible for Stp1p processing. It has been suggested that a similar mechanism involving an Ssy5p-like protein might operate in *Y. lipolytica* (Gonzalez-Lopez et al. 2002). It will be interesting to determine if YlOpt1p and YlSsy5p are part of the same signaling pathway.

YlSSY5 (YALI0E04400g) has strong homology to *ScSSY5* (6e-88). The His, Asp, and Ser triad characteristic of the serine protease active site and surrounding residues is highly conserved, as is its putative self-endoproteolytic processing site (Abdel-Sater et al. 2004). The best candidate for *YlPTR3* is YALI0D02673g with two non-overlapping homologous regions—(2e-45; 85/218) and (2e-21; 93/190). The best candidates for *YlSSY1*, YALI0B19338g (2e-66) and YALI0C00451g (9e-63), and for *YlSTP1*, YALI0E24937g (1e-36) and YALI0B05478g (8e-20), are not as convincing.

In conclusion, progress has been significant on pH and *XPR2* regulation, including some on protein/peptide induction.

6 *AXP1* Regulation

Compared to *XPR2*, much less is known about *AXP1* regulation. AXP is produced during exponential growth. Production was higher with proteins and peptones than amino acids and ammonium ion (Yamada and Ogrydziak 1983). The effects of C- and S-availability have not been specifically studied. *AXP1* expression is also regulated by pH. *AXP1* mRNA expression was maximum at pH 5.5 and decreased as neutral pH was approached (Glover et al. 1997). There are three copies of the core PacC hexanucleotide in the *AXP1* promoter (Lambert et al. 1997).

pH regulation was studied using continuous cultures and pH-controlled batch cultures (Glover et al. 1997). *AXP1* mRNA was found from pH 4.5–6.5 and *XPR2* mRNA from pH 5.5–7.5. At alkaline pH, a strong band for *XPR2* and no discernible band for *AXP1*, and at acidic pH, a strong band for *AXP1* and no discernible band for *XPR2*, were found on Northern blots for pH 6.8 versus pH 4.5 (Lambert et al. 1997) and pH 7.0 versus 4.0 (Gonzalez-Lopez et al. 2002).

In the batch culture, AEP activity was produced at pH as low as 5.0 where there was little *XPR2* mRNA. The drop off in AXP activity was faster than for *AXP1* mRNA levels at pH 6.5 and pH 7.0. Glover et al. (1997) suggested that AXP may be degraded by AEP at these pHs. Surprisingly, stability of AEP to AXP and vice versa at different pHs has never been directly measured using purified enzymes.

The Rim pathway is involved in *AXP1* regulation. The model, explored in the most detail in *A. nidulans*, is that activated (C-truncated) Rim101p would be predicted to induce alkaline genes such as *XPR2* and to repress acidic genes such

as *AXP1* at neutral/alkaline pH. Unexpectedly, if the Rim pathway is disrupted, *AXP1* is not expressed at pH 7.0 (Gonzalez-Lopez et al. 2002). It was proposed that at pH 7.0, where AXP is inactive, induction cannot occur because production of a specific *AXP1* inducer is dependent on AEP activity.

The model predicts that at acidic pH, little or no Rim101p is activated and alkaline genes are not induced and acidic genes not repressed. As predicted, no *XPR2* mRNA was detected at pH 4.0. Surprisingly, when the Rim pathway was disrupted, reduced levels of *AXP1* mRNA were detected at pH 4.0 compared to wild type suggesting that under acidic conditions full induction of *AXP1* requires the Rim pathway (Gonzalez-Lopez et al. 2002). The authors proposed that induction of *AXP1* is not dependent on Rim pathway for pH sensing but for interpretation of other signals, possibly nutrient limitation.

Both *ssy5* and *opt1* mutants make no *AXP1* mRNA at pH 4.0 suggesting that the signaling pathway(s) involving these genes has a role in *AXP1* expression.

7 Heterologous Protein Expression

Extracellular proteases have played a major role in heterologous protein production. The *XPR2* prepro-region has provided localization and processing signals. Heterologous expression using p*XPR2* in a *Δaxp1 Δxpr2* host was commonly done using YPDm medium at pH 6.8. The host cannot degrade the proteins in YPDm. However, 5.0 % PP provides enough low molecular weight C- and N-sources for cell growth. When these become limiting late in log phase, growth slows, p*XPR2* is induced, and heterologous protein expression starts. In contrast, for Xpr2+ strains growing in medium with lower levels of PP, AEP production starts early in log phase and basically stops in stationary phase.

Minimal medium is less expensive than YPDm, and it simplifies product purification from undegraded proteins and peptides. UAS1B hybrid promoters were less affected by environmental conditions, and a promoter consisting of four UAS1B fragments with a minimal downstream region from p*LEU2* made use of minimal media possible (Madzak et al. 2000). Expression was quasi-constitutive in minimal MMAm medium and 60–85 % of that for native p*XPR2* on YPDm medium.

8 Other Extracellular Proteases

The MEROPS Peptidase Database (Release 9.1) was used to predict potential extracellular proteases in *Y. lipolytica* CLIB122 (Rawlings et al. 2010). There are 131 known and putative peptidase entries. The MEROPS definition of peptidases includes broad specificity endoproteinases (emphasized in this chapter) and exopeptidases that remove one or two amino acids at a time. The entries were screened for signal peptides using SignalP 3.0. Proteins predicted to have signal

peptides by both NN and HMM (probability ≥0.900) were considered to be potentially secreted.

MEROPS defines 12 peptidase families and reports frequency of family members versus frequency in genomes of the other sequenced fungi. In *Y. lipolytica*, three families had undergone lineage-specific expansion. *Y. lipolytica* has 34 homologs in A1 (pepsin family)—endoproteinases, usually active at acidic pH, with an aspartic active site. The next highest is *Neurospora crassa* with 18, and *S. cerevisiae* has only 11. *Y. lipolytica* has 19 homologs in the S8 (subtilisin family)—peptidases homologous to the serine endoproteinase subtilisin. *N. crassa* has 10 and *S. cerevisiae* 11. The third expanded family is the serine carboxypeptidase family S10.

Family A1 includes *AXP1* and has 30 potentially secreted members (Table 1). Two had strongest homology to *ScPEP4* and are probably vacuolar. Fourteen had strongest homology to *S. cerevisiae* yapsin and may be GPI anchored at the cell surface. And one had strongest homology to *ScBAR1*.

YALI0E33363g (blastp score of 1e-92) and YALI0D10967g (2e-88) were most similar to *AXP1* (YALI0B05654g) in sequence and predicted protein size. For all three, the predicted signal peptide cleavage site was identical, the next two amino acids were Ala.Pro, and a Phe.Ala autoprocessing site was similarly located. Based on microarray analysis of AEP induction in strains carrying multiple copies of *XPR2* (see below), *AXP1* and YALI0E33363g provided sufficient signal to determine expression ratios at all time points but YALI0D10967G only at one. It may be poorly expressed under these conditions.

There is a large drop off in sequence homology with YALI0B20526g (3e-31) as next highest. Of the 30 pepsin-like genes coding for potentially secreted proteases, 21 provided sufficient signal at all time points to determine expression ratios. The nine remaining genes might be expressed in other conditions.

Four genes (not included in MEROPS) that code for potentially secreted pepsin-like proteins with the characteristic catalytic active site were identified. Three had strongest homology to *S. cerevisiae* yapsin and all weak homology to *AXP1*.

Yamada and Ogrydziak (1983) found three extracellular acid proteases, but Nelson and Young (1987) found only one. The three proteases were separated by ion exchange chromatography and had similar molecular masses—40.3–40.7 kDa—determined by SDS-PAGE. Carbohydrate contents were 25 %, 12 %, and 1.2 % for proteases I, II, and III, respectively. Isoelectric point was 3.8 for protease III and 4.9 for protease I. Based on molecular mass, isoelectric point, and carbohydrate content, protease III corresponds to AXP. Arguments in favor of proteases YALI0E33363p and YALI0D10967p being proteases I and II are similar predicted masses of the mature molecules (37.4–37.9 kDa) and AXP-like location for potential Phe-Ala autoprocessing sites. Also the predicted isoelectric point for mature YALI0D10967p is 4.9, identical to that of protease I. An argument against identity of these proteases is that YALI0E33363p has no potential N-linked glycosylation site and YALI0D10967p only one. If carbohydrate content differences were due to O-linked glycosylation, then SDS-PAGE mobility should differ significantly. Therefore, identity would require that the reported carbohydrate contents of

Table 1 A1 family—potentially secreted pepsin-like proteases

Gene	**Name**[a] Homolog	MEROPS	blastp versus *AXP1*	Amino acids	Signal peptide cleavage site NN	Signal peptide cleavage site HMM	Microarray data[b]
YALI0B05654g	***AXP1***	MER003667	0.0	397	17–18	17–18	Yes
YALI0E33363g		MER101133	1e-92	397	17–18	17–18	Yes
YALI0D10967g		MER175599	2e-88	403	17–18	17–18	No
YALI0B20526g	*Ct ASP*	MER101142	3e-31	392	20–21	20–21	No
YALI0C20273g	*CtASP2*	MER101138	2e-28	385	17–18	26–27	No
YALI0D14300g	*ScYPS3*	MER101135	8e-28	384	17–18	17–18	Yes
YALI0A02002g	*ScYPS3*	MER101143	5e-27	443	22–23	22–23	No
YALI0B00374g	*S. fib.* ASP	MER101140	7e-27	389	18–19	23–24	Yes
YALI0F10549g	*ScYPS3*	MER101130	2e-24	450	17–18	17–18	Yes
YALI0E25784g	*CtASP4*	MER177669	1e-23	393	17–18	17–18	Yes
YALI0B00132g	*S. fib.* ASP		8e-23	476	17–18	23–24	Yes
YALI0C08547g	*CaASP3*	MER101137	2e-22	385	17–18	17–18	No
YALI0E10175g	*ScYPS3*	MER071463	2e-21	534	17–18	17–18	Yes
YALI0D01331g	*ScYPS3*	MER184679	4e-20	457	17–18	17–18	Yes
YALI0B20174g	*ScYPS3*	MER101141	6e-19	393	17–18	17–18	Yes
YALI0D10835g	*A. ory* ASP	MER175569	3e-17	778	18–19	18–19	Yes
YALI0F27071g	*ScPEP4*	MER107343	8e-17	396	18–19	18–19	Yes
YALI0C14938g	*ScYPS3*	MER184465	1e-16	447	17–18	17–18	Yes
YALI0E22374g	*ScYPS3*	MER071464	2e-15	727	15–16	15–16	Yes
YALI0D17270g	*ScYPS3*		8e-14	391	14–15	18–19	No
YALI0C08899g	*CtASP4*	MER184463	1e-13	359	18–19	18–19	Yes
YALI0E13860g	*ScYPS3*	MER101131	3e-13	378	20–21	20–21	No
YALI0D22957g	*ScYPS3*	MER184467	7e-13	455	17–18	22–23	No
YALI0A16819g	*CaASP4*	MER172235	1e-11	457	18–19	18–19	Yes
YALI0F09163g	*ScYPS3*		3e-11	388	23–24	23–24	Yes
YALI0C10923g	*ScYPS3*		1e-09	416	14–15	25–26	Yes
YALI0D02024g	*ScPEP4*	MER101134	6e-09	625	17–18	17–18	Yes
YALI0C10135g	*ScYPS3*	MER184405	4e-08	411	13–14	16–17	Yes
YALI0C08283g	*CtASP4*	MER101136	9e-07	374	15–16	20–21	No
YALI0E11715g	*ScBAR1*	MER184468	>7.7	394	18–19	18–19	Yes

[a]Gene name is in bold. *Ct*, *Candida tropicalis*; *Sc*, *S. cerevisiae*; *S. fib.*, *Saccharomycopsis fibuligera*; *Ca*, *Candida albicans*; *A. ory.*, *Aspergillus oryzae*; ASP, acid secreted protease
[b]Expressed in AEP induction conditions based on microarray data

proteases I and II be incorrect. Also *Δaxp1* strains made no zone of clearing on BSA (pH 4.0) plates (Otero and Gaillardin 1996). YALI0D10967p and YALI0E33363p would have to be expressed at sufficiently low levels on these plates that no zones of clearing could be detected.

Family S8 includes *XPR2* (YALI0F31889g) and has 16 potentially secreted members (Table 2). Of these, two had strongest homology with *ScPRB1* and with each other (e-170) and may be vacuolar, and one was Xpr6p thought to be Golgi located. YALI0A08360g (not in MEROPS) has strong sequence similarity (5e-98) with *XPR2* including the Asp, His, and Ser catalytic triad.

Table 2 S8 family—potentially secreted subtilisin-like proteases

Gene	**Name**[a] Homolog	MEROPS	blastp versus *XPR2*	Amino acids	Signal peptide cleavage site NN	Signal peptide cleavage site HMM	*XPR6* site	Microarray data[b]
YALI0F31889g	***XPR2***	MER000340	0.0	454	15–16	21–22	Yes	Yes
YALI0D02981g		MER191803	1e-167	450	15–16	21–22	Yes	Yes
YALI0A09262g	***AEP2***	MER055295	1e-102	544	15–16	15–16	No	Yes
YALI0A08360g			5e-98	533	15–16	15–16	No	Yes
YALI0B22880g		MER191800	1e-80	467	15–16	20–21	Yes	Yes
YALI0B19316g		MER191799	3e-74	453	23–24	15–16	No	Yes
YALI0C15532g		MER191801	3e-71	892	19–20	19–20	No	No
YALI0E28875g		MER191804	9e-66	475	16–17	16–17	Yes	Yes
YALI0C20691g		MER191802	4e-61	512	19–20	19–20	No	Yes
YALI0A10208g		MER167710	3e-58	419	17–18	17–18	No	No
YALI0B16500g	*ScPRB1*	MER191798	1e-55	516	18–19	18–19	No	Yes
YALI0A06435g	*ScPRB1*	MER167615	6e-48	471	16–17	18–17	No	Yes
YALI0F19646g		MER191806	1e-46	415	14–15	19–20	No	No
YALI0B02794g	*Dh* SP	MER191797	1e-39	379	19–20	19–20	No	Yes
YALI0F24453g	*Ca* SP	MER191807	7e-37	440	15–16	15–16	No	No
YALI0F13189g	***XPR6***	MER000366	5e-01	976	17–18	17–18	–	Yes

[a]Gene name is in bold. *Sc*, *S. cerevisiae*; *Dh*, *Debaryomyces hansenii*; *Ca*, *Candida albicans*; *SP*, serine protease

[b]Expressed in AEP induction conditions based on microarray data

YALI0D02981g has strongest homology to *XPR2* (e-167). The sizes are very similar, the predicted signal peptide cleavage sites are identical, there are four X-Ala, X-Pro dipeptides versus nine for AEP, and N-linked glycosylation and dibasic processing (Lys.Arg) sites appear in similar locations.

YALI0A09262g (AEP2) (e-102) and YALI0A08360g (5e-98) are the next closest homologs to *XPR2*. They are more closely related in size and sequence (1e-0.0) to each other than to *XPR2*. Like *XPR2*, the predicted signal peptide cleavage sites are 15–16. Neither has an N-linked glycosylation or Lys.Arg site in appropriate locations to mimic AEP processing.

YALI0B22880g has similar size and the next strongest homology (1e-80). It has identical predicted signal peptide cleavage site (15–16) using NN and near identical (20–21 versus 21–22) using HMM. Both a potential N-linked glycosylation and Lys.Arg sites are in similar locations compared to AEP.

Except for YALI0C15532g, the remaining nine potentially secreted S8 family proteins are similar in size to AEP. Blastp scores range from 7e-37 to 3e-74. Only one had the 15–16 signal peptide cleavage site. None had the appropriately located N-linked glycosylation and Lys.Arg processing sites.

It is not known how many of this S8 family are actually expressed and secreted. In microarray experiments (see below), only four did not provide sufficient signal to determine expression ratios at all time points. Starting with only the sequencing information, it would have been a daunting task to knock out all the potentially

secreted S8 family member genes to stabilize secreted heterologous proteins. However, *Δxpr2* strains make no zone of clearing on SKM plates (pH 6.8), and including *Δxpr2* in host strains seems sufficient to largely stabilize secreted heterologous proteins. *AEP2* has been disrupted in a *Δxpr*2 background, and no phenotypic difference for heterologous protein production was observed (J.Y. Kim, personal communication).

The remaining potentially secreted peptidases were primarily amino- and carboxypeptidases but also included homologs to peptidases involved in mating factor processing.

It would be interesting to determine how expression of S8 family members is regulated, where they are located, and their biological roles.

9 Regulation of Secretory Pathway Components

Synonymous codon usage was more biased for *Y. lipolytica* than for *S. cerevisiae* for genes involved in protein targeting and secretion, suggesting that *Y. lipolytica* might produce these components at much higher levels. The hypothesis that *Y. lipolytica* may regulate components of the secretory pathway in response to secretory demand was tested by overexpressing AEP and measuring changes in genomic transcription.

9.1 Construction and Screening of XPR2 *Multicopy Strains*

Multiple copies of *XPR2* can be integrated by targeting plasmid pINA773 (containing *XPR2*, *URA3d* with a greatly truncated promoter, a fragment of *Y. lipolytica* rDNA, and a pBR322 fragment) to rDNA (Le Dall et al. 1994). Because of the truncated promoter, only multicopy integrants make enough Ura3p to support growth. Strains with 25–60 copies of *XPR2* were transferred from a rich medium at pH 4.0 (*XPR2* is repressed) to a glucose/proteose peptone (GPP) medium at pH 6.8. The strains grew rapidly for 10–11 h, but then AEP was induced and growth slowed for several hours before increasing again. By this time *XPR2* copy numbers had decreased.

To avoid loss of *XPR2* gene copies, a method for more rapid induction was developed. Major modifications were to induce at 23 °C where AEP differential productivity ((ΔUnits/ml)/(Δcell dry weight/ml)) is highest (Dedeoglu, E., unpublished results) and to replace PP with a 90 % dialyzed PP/10 % PP mixture. This removed most of the low molecular weight N-compounds that repress *XPR2* expression. In the new induction conditions, AEP production for strain 773–2 (containing 40–50 copies of *XPR2*) had started an hour after transfer and growth slowed by 3 h. Considering the short time and that cell mass had increased less than 50 % at 3 h, little decrease in *XPR2* copy number should have been possible.

Strain CX161-1B grew more rapidly, produced more AEP, and had higher cell yields than 20–12, parent of 773–2 (unpublished data). Also growing inoculum in a defined synthetic complete (SC) medium at pH 6.8 with ammonia as the N-source would more reliably repress AEP synthesis and avoid the large pH change (4.0–6.8) on induction. Both 20–12 and 773–2, related to inbred E129 strains, utilize ammonia very poorly. Therefore, *XPR2* multicopy strains were constructed with a CX161-1B-related strain as parent. These strains grew more slowly than expected in SC medium. W29 (isolated from the sewers of Paris) produced slightly more AEP and grew much better in SC medium than CX161-1B (unpublished results). Therefore, W29-related *XPR2* multicopy strains and additional CX161-1B *XPR2* multicopy strains were constructed.

About 200 transformants were prescreened by streaking on YLT-ura plates (SC supplemented with amino acids and nucleotides). AEP production of 64 isolates was estimated by measuring the diameters of colonies and zones of clearing for cells spotted on SKM plates. Growth on YLT-ura plates was estimated by colony diameter. Plates were incubated at 23 °C and measurements done every 24 h.

The diameters of zones of clearing and colonies on SKM plates were slightly larger for W29 compared to CX161-1B. For *XPR2* multicopy W29 transformants, zones of clearing were comparable to those for parental W29, but colony diameters were always smaller, consistent with the *XPR2* multicopy strains producing more AEP per cell. Colony sizes on YLT-ura were slightly larger for W29 than CX161-1B. For most of the *XPR2* multicopy transformants, colonies on YLT-ura were noticeably smaller than for the parents.

AEP activity can be estimated by measuring the zones of clearing on SKM plates around wells filled with liquid samples. The logarithm of AEP concentration is linearly related to the diameter of the zone of clearing (Ogrydziak and Scharf 1982). AEP production was estimated using the diameter of the zone of clearing around the colony and the log conversion. Colonies were disc shaped, and cell numbers were estimated from the area. Fifteen transformants were screened several times. The eight producing the highest levels of AEP were screened further in liquid culture. All were derived from W29.

Cells were grown overnight in defined medium at pH 6.8 and resuspended at ~1 g/L dry weight cells in induction medium in flasks incubated at 23 °C. Klett readings, AEP well assays on SKM plates, and pH measurements were done. Strains 3 and 44 were chosen for further study. Compared to W29, AEP production by strain 3 was 6-fold higher at 12 h and 12.4-fold higher at 24 h. These were among the highest values. The increase in AEP production of strain 44 compared to W29 (6.2-fold) was similar to that for strain 3 at 12 h and somewhat lower (9.2-fold) at 24 h. However, growth after transfer of strain 44 slowed the least of any of the high-producing transformants. Significant AEP overproduction combined with more wild type-like growth rates would be of interest because some changes in gene expression after AEP induction may not be specific for secretion stress but due to decreases in growth rate.

9.2 AEP Levels

Ten hours after transfer, AEP production (AEP-related protein/dry cell weight) for W29 is about 2.3 % of total protein. This is calculated using 9,000 U = 1 mg of AEP (Ogrydziak and Scharf 1982), a 1.486 mass ratio of pro-mAEP (the propeptide is also secreted) to mAEP, and the assumption that cells are 50 % protein. The differential rate of AEP production ((ΔAEP-related protein/ml)/(Δcell protein/ml)) varied from 3.8 to 3.2 % over 10 h.

For strain 3 at 10 h, average pro-mAEP production was 5.6 %. At 24 h, it was 11.5 %. Values were much higher for differential rates of pro-mAEP production—16.4 % for 0–3 h and as high as 29.3 % for 16–28 h.

Estimating secretory stress on a cell is difficult. Even when cells are not secreting proteins into the extracellular medium, there is substantial traffic through the secretory pathway to support cell growth. The percentage of total protein synthesized that enters the secretory pathway is unknown. If it were 30 % and if AEP is 10–15 % of total protein synthesized, then AEP induction would increase secretory demand by 33–50 %. Heterogeneity of AEP production from cell to cell would result in heterogeneity of secretion stress. In any case, for strain 3, AEP induction leads to slowing of cell growth (td of 8.5 h from 3 to 7 h versus 3.6 h for W29 over the same time period) and a decrease of the differential rate of AEP production after 3 h.

For strain 44 at 10 h, average pro-mAEP production was 9.4 %. Differential rates were 11.4 % for 0–3 h, 12.1 % for 3–6 h, and as high as 20.6 % for 8–10 h. Differential rates were lower than for strain 3 from 0 to 3 h, actually slightly increased after 3 h, and growth did not slow as much (td of 4.1 h from 3 to 7 h).

9.3 Transcriptional Response to Secretion Stress

A DNA microarray experiment was done to determine what genes responded to secretion stress. Cells were transferred to AEP induction medium and samples taken at various times. For strain 3, based on quality/quantity of the RNA preparations, growth rates, and AEP levels, the 1.5, 4, 6, 12, 16, and 24 h samples were used. For strain 44, 2, 4, 6, 7, and 9 h samples were used. The earliest time point (control) was not taken right after transfer but when AEP was already induced and before growth had slowed. Comparison of gene expression levels when growth starts to slow with this time point was expected to more specifically address how cells adapt to secretion stress.

Genes were considered to be differentially expressed based on SAM analysis (Tusher et al. 2001), EDGE analysis (Leek et al. 2006), or if at least three time points had a threefold difference in expression. There was data for at least three times points for 5,915 genes for strain 3 and 5,216 genes for strain 44. Fifty genes were induced in both strains. For strains 3 and 44, 84 and 62 genes were uniquely induced, respectively.

For both strains, none of the ten most strongly induced genes at 4 h were secretory pathway genes. Some make biological sense—an ammonium transporter and two vacuolar proteases. Most presently do not.

The only induced secretory pathway-related genes are homologs of *VPS13*, *SSA4*, and *SSO1*, and induction was strongest at later time points. Overexpression in *S. cerevisiae* of *S. cerevisiae* and *K. lactis SSO1* homologs, plasma membrane t-SNAREs involved in secretory vesicle fusion, enhanced production of secreted proteins, suggesting they may be a rate-limiting components for protein secretion (Toikkanen et al. 2004). Four potential transcription factors were induced—*HOY1*, *RIM101*, and homologs of *ScCAT8* and ScGZF3—but again induction was strongest at later time points.

Besides *XPR2*, several potentially secreted proteases were induced—the *ScPRB1* homolog (YALI0B16500g) in both strains and the *ScPEP4* homolog (YALI0F27071g) in strain 44. The *ScBAR1* homolog (YALI0B00374g) was induced in strain 3 and YALI0A08360g (more closely related to *AEP2* than *XPR2*) in strain 44.

The differentially expressed genes were analyzed by GO Term Finder (http://go.princeton.edu/cgi-bin/GOTermFinder); it identifies significantly enriched genes in a list of genes. This is not possible directly in *Y. lipolytica*. Therefore, *S. cerevisiae* genes with blastp score $\leq$1e-20 against their *Y. lipolytica* homologs were included in the gene list and analyzed against overall GO term frequencies for *S. cerevisiae*. As discussed above, gene frequencies for certain classes of genes can differ significantly between the two yeasts. Of the 50 genes induced in both strains, 31 met the criterion. Cation transport was the only process ontology term enriched. Six genes were annotated to the term including two ammonium permeases.

For strain 44, of the 112 genes induced, 71 made the list. Transmembrane transport was the only process ontology term enriched. Fourteen genes were annotated to the term including nine transporters of low molecular weight N-sources.

Eighty of 134 genes induced in strain 3 made the list. Fifteen process ontology terms were enriched. The same 18 genes were annotated to four terms including carboxylic acid, oxoacid, cellular ketone, and organic acid metabolic processes. Eleven genes were annotated to ion transport including zinc, copper, and lactate transporters and three involved with ammonium, also annotated to nitrogen utilization and ammonium transport. Thirteen genes were annotated to response to abiotic stress including *ATG8*, *PRB1*, *CTT1*, and *HSP31*.

Far more genes (250) were repressed in both strains. For strains 3 and 44, 229 and 74 genes were uniquely repressed, respectively. For both strains, the ten most repressed genes at 4 h had no obvious connection to protein secretion. No potentially secreted proteases were repressed, and three transcription factors (*MHR1*, *YDR296W* and *ZPR1*) were repressed in both strains. Several heat shock genes, cochaperones, and *EGD1* and *EGD2* (nascent polypeptide-associated complex (NAC) subunits involved in protein targeting) were repressed in both strains. In strain 3, unexpectedly *SRP21* and *SRP14*, components of the signal recognition particle, were also repressed. In strain 44, *SEC61*, a component of the translocon was repressed.

Many of the repressed genes corresponded to genes whose expression level was positively correlated with growth rate in *S. cerevisiae* (Brauer et al. 2008), suggesting that their repression is a response to the slower growth rate and not specific for secretion stress. GO analysis terms were enriched in genes involved in ribosomal (both mitochondrial and cytosolic) biogenesis and assembly, ribosomal constituents, rRNA processing, translation, and mitochondrial protein import.

More genes are repressed than induced after AEP induction in *XPR2* multicopy strains. Unfortunately, the time points chosen did not allow an unambiguous answer to the question of whether or not the unfolded protein response (Ron and Walter 2007) is induced. Surprisingly, for strain 3 the increase in *XPR2* expression was only two- to threefold at earlier time points, and for strain 44 there was little increase in expression. The ten genes with the highest average fluorescent intensity at the earliest time point (control) were identified. Although several factors may affect intensity, high intensity should reflect a high mRNA level. *XPR2* ranked first for strain 44 and first or second (depending on the chip) for strain 3, suggesting that *XPR2* was already highly expressed and almost fully induced in the control samples.

KAR2 and *PDI1* are induced in UPR. Except for the 4 h sample for strain 44, there was no evidence of induction of these two genes. For strain 3, there was evidence of repression for *KAR2* at later time points. However, for strain 3 *KAR2* ranked seventh for average fluorescent intensity at 1.5 h, again suggesting it was already almost fully induced. *PDI1* appears to be expressed at more moderate levels. Unfortunately, much of the evidence for UPR-like response may have been missed if it had already occurred when the control sample was taken. It is possible that UPR and other responses to secretion stress such as increases in ER and translocon components had already happened. The repression of *SEC61*, *SRP14*, and *SRP21* and induction of the autophagy gene *ATG8* and vacuolar proteases *PRB1* and *PEP4* might reflect a turning down of this response. It would be interesting to (1) use an earlier control sample and examine more closely spaced time points, (2) follow AEP induction in a strain with a single copy of *XPR2*, and (3) determine if ER had increased as part of the response.

References

Abdel-Sater F, El Bakkoury M, Urrestarazu A, Vissers S, Andre B (2004) Amino acid signaling in yeast: casein kinase I and the *Ssy5* endoprotease are key determinants of endoproteolytic activation of the membrane-bound Stp1 transcription factor. Mol Cell Biol 24:9771–9785

Ahearn DG, Meyers SP, Nichols RA (1968) Extracellular proteinases of yeasts and yeastlike fungi. Appl Microbiol 16:1370–1374

Barth G, Gaillardin C (1996) *Yarrowia lipolytica*. In: Wolf K (ed) Non-conventional yeasts in biotechnology a handbook. Springer, Berlin, pp 313–388

Bendtsen JD, Nielsen H, von Heijne G, Brunak S (2004) Improved prediction of signal peptides: SignalP 3.0. J Mol Biol 340:783–795

Blanchin-Roland S, Cordero Otero RR, Gaillardin C (1994) Two upstream activation sequences control the expression of the *XPR2* gene in the yeast *Yarrowia lipolytica*. Mol Cell Biol 14:327–338

Blanchin-Roland S, Da Costa G, Gaillardin C (2005) ESCRT-I components of the endocytic machinery are required for Rim101-dependent ambient pH regulation in the yeast *Yarrowia lipolytica*. Microbiology 151:3627–3637

Brauer MJ, Huttenhower C, Airoldi EM, Rosenstein R, Matese JC, Gresham D, Boer VM, Troyanskaya OG, Botstein D (2008) Coordination of growth rate, cell cycle, stress response, and metabolic activity in yeast. Mol Biol Cell 19:352–367

Davidow LS, O'Donnell MM, Kaczmarek FS, Pereira DA, DeZeeuw JR, Franke AE (1987) Cloning and sequencing of the alkaline extracellular protease gene of *Yarrowia lipolytica*. J Bacteriol 169:4621–4629

Enderlin CS, Ogrydziak DM (1994) Cloning, nucleotide sequence and functions of *XPR6*, which codes for a dibasic processing endoprotease from the yeast *Yarrowia lipolytica*. Yeast 10:67–79

Fabre E, Tharaud C, Gaillardin C (1992) Intracellular transit of a yeast protease is rescued by trans-complementation with its prodomain. J Biol Chem 267:15049–15055

Glover DJ, McEwen RK, Thomas CR, Young TW (1997) pH-regulated expression of the acid and alkaline extracellular proteases of *Yarrowia lipolytica*. Microbiology 143(Pt 9):3045–3054

Gonzalez-Lopez CI, Szabo R, Blanchin-Roland S, Gaillardin C (2002) Genetic control of extracellular protease synthesis in the yeast *Yarrowia lipolytica*. Genetics 160:417–427

Hu Z, Haghjoo K, Jordan F (1996) Further evidence for the structure of the subtilisin propeptide and for its interactions with mature subtilisin. J Biol Chem 271:3375–3384

Lambert M, Blanchin-Roland S, Le Louedec F, Lepingle A, Gaillardin C (1997) Genetic analysis of regulatory mutants affecting synthesis of extracellular proteinases in the yeast *Yarrowia lipolytica*: identification of a RIM101/pacC homolog. Mol Cell Biol 17:3966–3976

Le Dall MT, Nicaud JM, Gaillardin C (1994) Multiple-copy integration in the yeast *Yarrowia lipolytica*. Curr Genet 26:38–44

Leek JT, Monsen E, Dabney AR, Storey JD (2006) EDGE: extraction and analysis of differential gene expression. Bioinformatics 22:507–508

Madzak C, Blanchin-Roland S, Cordero Otero RR, Gaillardin C (1999) Functional analysis of upstream regulating regions from the *Yarrowia lipolytica XPR2* promoter. Microbiology 145 (Pt 1):75–87

Madzak C, Treton B, Blanchin-Roland S (2000) Strong hybrid promoters and integrative expression/secretion vectors for quasi-constitutive expression of heterologous proteins in the yeast *Yarrowia lipolytica*. J Mol Microbiol Biotechnol 2:207–216

Matoba S, Ogrydziak DM (1989) A novel location for dipeptidyl aminopeptidase processing sites in the alkaline extracellular protease of *Yarrowia lipolytica*. J Biol Chem 264:6037–6043

Matoba S, Ogrydziak DM (1998) Another factor besides hydrophobicity can affect signal peptide interaction with signal recognition particle. J Biol Chem 273:18841–18847

Matoba S, Fukayama J, Wing RA, Ogrydziak DM (1988) Intracellular precursors and secretion of alkaline extracellular protease of *Yarrowia lipolytica*. Mol Cell Biol 8:4904–4916

Matoba S, Morano KA, Klionsky DJ, Kim K, Ogrydziak DM (1997) Dipeptidyl aminopeptidase processing and biosynthesis of alkaline extracellular protease from *Yarrowia lipolytica*. Microbiology 143(Pt 10):3263–3272

McEwen RK, Young TW (1998) Secretion and pH-dependent self-processing of the pro-form of the *Yarrowia lipolytica* acid extracellular protease. Yeast 14:1115–1125

Nelson G, Young TW (1987) Extracellular acid and alkaline proteases from *Candida olea*. J Gen Microbiol 133:1461–1469

Ng DT, Brown JD, Walter P (1996) Signal sequences specify the targeting route to the endoplasmic reticulum membrane. J Cell Biol 134:269–278

Nicaud J-M, Fabre E, Beckerich JM, Fournier P, Gaillardin C (1989) Cloning, sequencing and amplification of the alkaline extracellular protease (*XPR2*) gene of the yeast *Yarrowia lipolytica*. J Biotechnol 12:285–297

Ogrydziak DM (1993) Yeast extracellular proteases. Crit Rev Biotechnol 13:1–55

Ogrydziak DM, Mortimer RK (1977) Genetics of extracellular protease production in *Saccharomycopsis lipolytica*. Genetics 87:621–632

Ogrydziak DM, Scharf SJ (1982) Alkaline extracellular protease produced by *Saccharomycopsis lipolytica* CX161-1B. J Gen Microbiol 128:1225–1234

Ogrydziak DM, Demain AL, Tannenbaum SR (1977) Regulation of extracellular protease production in *Candida lipolytica*. Biochim Biophys Acta 497:525–538

Otero RC, Gaillardin C (1996) Dominant mutations affecting expression of pH-regulated genes in *Yarrowia lipolytica*. Mol Gen Genet 252:311–319

Ozcan S, Dover J, Rosenwald AG, Wolf S, Johnston M (1996) Two glucose transporters in *Saccharomyces cerevisiae* are glucose sensors that generate a signal for induction of gene expression. Proc Natl Acad Sci USA 93:12428–12432

Rawlings ND, Barrett AJ, Bateman A (2010) MEROPS: the peptidase database. Nucleic Acids Res 38:D227–D233

Ron D, Walter P (2007) Signal integration in the endoplasmic reticulum unfolded protein response. Nat Rev Mol Cell Biol 8:519–529

Sherman DJ, Martin T, Nikolski M, Cayla C, Souciet JL, Durrens P (2009) Genolevures: protein families and synteny among complete hemiascomycetous yeast proteomes and genomes. Nucleic Acids Res 37:D550–D554

Thevenieau F, Nicaud J-M, Gaillardin C (2009) Applications of non-conventional yeast *Yarrowia lipolytica*. In: Satyanarayana T, Kunze G (eds) Yeast biotechnology: diversity and applications. Springer, Dordrecht, pp 580–613

Toikkanen JH, Sundqvist L, Keranen S (2004) Kluyveromyces lactis *SSO1* and *SEB1* genes are functional in *Saccharomyces cerevisiae* and enhance production of secreted proteins when overexpressed. Yeast 21:1045–1055

Tusher VG, Tibshirani R, Chu G (2001) Significance analysis of microarrays applied to the ionizing radiation response. Proc Natl Acad Sci USA 98:5116–5121

Yamada T, Ogrydziak DM (1983) Extracellular acid proteases produced by *Saccharomycopsis lipolytica*. J Bacteriol 154:23–31

Yaver DS, Matoba S, Ogrydziak DM (1992) A mutation in the signal recognition particle 7S RNA of the yeast *Yarrowia lipolytica* preferentially affects synthesis of the alkaline extracellular protease: in vivo evidence for translational arrest. J Cell Biol 116:605–616

Young TW, Wadeson A, Glover DJ, Quincey RV, Butlin MJ, Kamei EA (1996) The extracellular acid protease gene of *Yarrowia lipolytica*: sequence and pH-regulated transcription. Microbiology 142(Pt 10):2913–2921

http://www.springer.com/978-3-642-38582-7

Yarrowia lipolytica
Biotechnological Applications
Barth, G. (Ed.)
2013, VII, 268 p., Hardcover
ISBN: 978-3-642-38582-7